Scientific Research Publishing

Open Journal of Applied Sciences, 2026, 16(1), 97-114
https://www.scirp.org/journal/ojapps
ISSN Online: 2165-3925
ISSN Print: 2165-3917

Disturbance of the Earth's Magnetosphere by High-Speed Solar Wind during Solar Cycle 24: Cross-Variability of MCEF and IMF-Bz and Assessment of Transmitted Power Using Wang's E_{int} Parameter

Kaboré Salfo[1*], Sawadogo Wambi Emmanuel[2], Sawadogo Abdoul-Mahaz[1], Madougou Saidou[3], Ouattara Frédéric[1]

[1]Laboratory of Analytical Chemistry, Space and Energy Physics (L@CAPSE), Norbert ZONGO University (UNZ), Koudougou, Burkina Faso
[2]Institut des Sciences et de Technologie (IST), Ecole Normale Supérieure (ENS), Ouagadougou, Burkina Faso
[3]Department of Physics, Ecole Normale Supérieure, University Abdou Moumouni, Niamey, Niger
Email: *salfo_kabore@yahoo.fr

How to cite this paper: Salfo, K., Emmanuel, S.W., Abdoul-Mahaz, S., Saidou, M. and Frédéric, O. (2026) Disturbance of the Earth's Magnetosphere by High-Speed Solar Wind during Solar Cycle 24: Cross-Variability of MCEF and IMF-Bz and Assessment of Transmitted Power Using Wang's E_{int} Parameter. *Open Journal of Applied Sciences*, **16**, 97-114.
https://doi.org/10.4236/ojapps.2026.161008

Received: October 2, 2025
Accepted: January 5, 2026
Published: January 8, 2026

Abstract

In this article, we analyse the response of the magnetospheric convection electric field (MCEF) and quantify the power transfer to the magnetosphere when it is disturbed by fast solar winds. Our dataset of 1-hour resolution solar winds and sunspots covers eleven years of OMNI and Silso data. We use the dynamic energy coupling function of Wang *et al.* (2014) to quantify the energy transfer during the different solar phases. We also use the relationship from Wu and Lei (1981), which we consider to be one of the best correlation formulas linking MCEF intensity and the solar electric field, to better estimate the MCEF response and its correlation with IMF-Bz. The study of the cross-variability of MCEF and IMF-Bz intensity shows that, regardless of the solar phase, the two fields evolve in opposition phase with very satisfactory correlations for each phase of solar cycle 24: −0.97 for the solar minimum and maximum phases, −0.99 for the ascending phase, −0.98 for the descending phase, and −0.98 regardless of the solar phase. It also appears that at any time of day, magnetic effects are ten to twenty times more prevalent in energy transfer phenomena between the magnetosphere and High-Speed Solar Wind than electrical effects. The power transmitted to the inner magnetosphere is minimal at the minimum phase (19 GW) and maximal during the descending phase (1096 GW). The power transmitted during the ascending phase (696 GW) is about

three times that transmitted during the solar maximum (216 GW). Regardless of the solar phase, the power transmitted to the inner magnetosphere is about 507 GW.

Keywords

High-Speed Solar Wind, Interplanetary Magnetic Field, Magnetospheric Convection Electric Field, Transmitted Power, Magnetosphere

1. Introduction

The Sun-Earth system is constantly interacting. Beyond gravitational interaction, the Sun interacts energetically and continuously with the upper layers of the atmosphere and the Earth's magnetosphere through the flow of magnetised particles from the Sun, known as solar wind: solar wind continuously feeds the magnetosphere of the Earth. The Earth's magnetosphere is a magnetic bubble that is essential for the preservation of life on Earth, particularly through its role as a shield, deflecting the highly energetic charged particles contained in the solar wind and cosmic rays, which would otherwise fall directly towards the Earth if they were not deflected. However, it is important to note that the Earth's magnetosphere is not completely impermeable, and small portions of solar wind particles (slow or fast) penetrate the magnetosphere on the night side through magnetic reconnection phenomena, but also through polar cones, which are magnetically neutral zones. These particles are then concentrated in the plasma sheet, where they undergo convection towards Earth. The different populations of solar wind particles that populate the inner magnetosphere are not independent and have different origins: ionosphere, solar winds, eruption particles, galactic and extra-galactic cosmic rays. They communicate with each other through a permanent large-scale circulation induced by an electric field known as the magnetospheric convection electric field (MCEF). Furthermore, it is a region where almost all the energy brought from the Sun in various forms (except electromagnetic) passes through to influence the ionosphere and thermosphere. It is also the place where several populations of particles of various origins "coexist" and interact with each other, giving rise to very complex and rich physics [1]. Finally, it is an extremely dynamic region, periodically subjected to violent magnetic storms, which originate in high-speed solar winds (HSSW). These HSSWs originate in coronal holes (CHs) or accompany interplanetary coronal mass ejections (ICMEs). The main manifestations of the disturbances caused by these solar winds are: ionisation of particles in the ionosphere; the production of substorms, magnetic storms and auroras. In addition to triggering the phenomenon of the aurora borealis, the high-energy particles that strike the Earth are also very harmful to humanity, capable of inflicting debilitating damage to communication satellites, electrical networks, submarine cables and aviation systems [2]-[4]. Resolving these failures caused by solar

events is often very costly, which has a negative impact on the global economy.

These findings lead us to investigate the characteristic mechanisms of magnetospheric dynamics during the different phases of solar cycle 24. The aim of this article is to study the response of the inner magnetosphere to high-speed solar winds (HSSW). This work will focus not only on magnetospheric convection due to fast solar wind plasma circulating in the inner magnetosphere, but also on the power transmitted to the inner magnetosphere during the interaction of this non-collisional magnetised plasma with geomagnetic lines. This investigation will illustrate different responses of the magnetospheric electric field and the energy dynamics of the magnetosphere to high-speed solar flux by phase of solar cycle 24, the last complete solar cycle and therefore the cycle for which the best investigative instruments were used. As our modern society has become increasingly dependent on reliable technologies, such as communication, navigation and power supply systems, which can be vulnerable to the influence of solar winds, monitoring and quantifying the energy transmitted by the solar wind to the inner magnetosphere will therefore contribute to a better understanding of how solar wind energy couples with the magnetosphere. This is essential in order to help create reliable weather forecasts. Ultimately, the aim of this research is therefore to contribute to providing information on the development of future forecasting capabilities for the power transmitted to the internal magnetosphere, with the ultimate goal of mitigating its impact on space and terrestrial technological systems. This will help, on the one hand, to accurately predict the effects of solar events on our planet and, on the other hand, enable engineers to properly define the manufacturing parameters of technological devices in order to reduce their likelihood of being damaged by solar events. In the rest of this study, in Sections 2 and 3, we present the data and methodology used, respectively. The results and discussions are presented in Section 4. We conclude this manuscript with a summary that not only recapitulates all our important results, but also outlines the limitations and different perspectives of this research.

2. Data

The following data were used in this scientific research:

- Solar wind parameters: fast solar wind velocities, fast solar wind density n, E_y component of the frozen electric field in the solar wind, and GSM coordinates of the B_x, By and Bz components of the interplanetary magnetic field (IMF). It is important to note that all of the solar wind parameters used in this study are available on the website http://omniweb.gsfc.nasa.gov/form/dx1.html.
- The annual number of sunspots available on the website: http://sidc.oma.be/sunspot-data/.

3. Methodology

3.1. Methods for Determining the Different Phases of Solar Cycles

To determine the four phases of each solar cycle using the sunspot number SN(t)

or Wolf index, we apply new criteria defined by [5] and used by [6]-[8] These criteria define the different phases of the solar cycle as follows:

(a) minimum phase: $SN(t) < 0.122 \times SN_{max}$;

(b) ascending phase: $0.122 \times SN_{max} \leq SN(t) \leq 0{,}73 \times SN_{max}$;

(c) phase maximum: $SN(t) > 0.73 \times SN_{max}$;

(d) descending phase: $0.73 \times SN_{max} \geq SN(t) > SN_{Min}$ (following cycle).

By applying these criteria different phases of the solar cycle 24 are identified as shown in Table 1.

Table 1. Illustration of the different phases of solar cycles 24 (extracted from [5]).

Cycle	Extension Period	Average Duration (years)	Minimum Phase	Ascending Phase	Maximum Phase	Descending Phase
24	2008-2018	11	2008-2009	2010-2011	2012-2014	2015-2018

3.2. Method for Determining High-Speed Solar Wind

In this scientific research, the criterion for identifying days with High-Speed Solar Wind speeds is based on the definition given by [9], according to whom a solar wind is considered fast if the daily average solar wind speed is greater than or equal to 450 km/s over at least two Bartels rotations. It is important to note that the definition of fast solar wind given by [10] [11] was improved by [9] later supported by several authors including [12] and [13] and used by [14]-[16]. The days on which the Earth's magnetosphere was impacted by fast solar winds are identified using eleven pixel diagrams (2008-2018) constructed from the average daily values of solar wind speed. Figure 1, which shows the pixel diagram for 2018, a year belonging to solar cycle 24, the subject of our study, illustrates a few days during which the Earth's magnetosphere was impacted by High-Speed Solar Wind (HSSW).

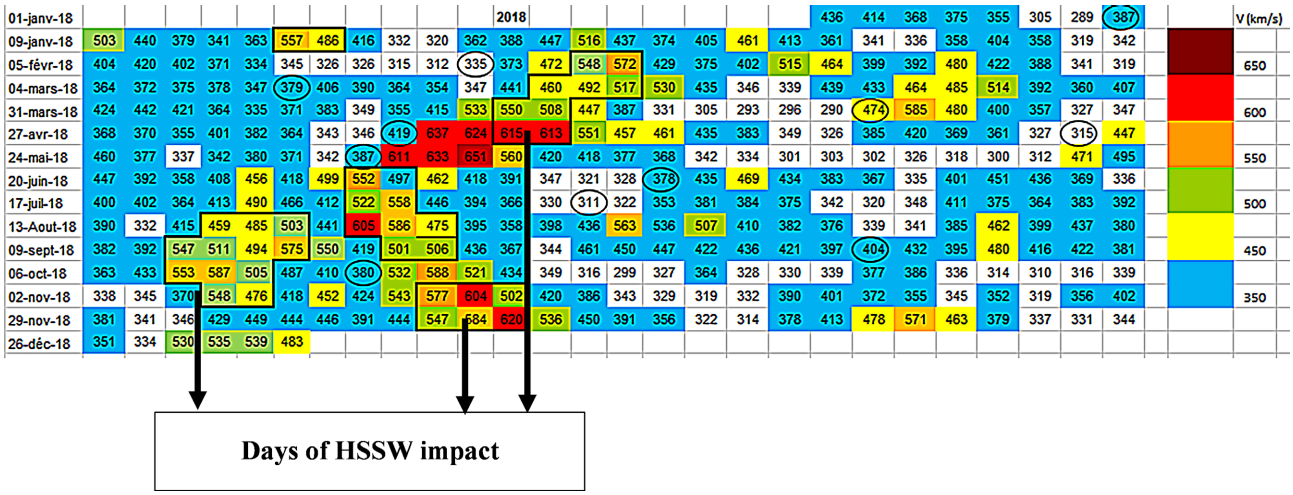

Figure 1. Pixel diagram for 2018 showing the days on which HSSW activities took place.

3.3. Method for Determining Solar Wind Parameters and the Intensity of the Magnetospheric Convective Electric Field (MCEF)

After identifying the dates on which the Earth's magnetosphere was subjected to rapid solar winds, we simultaneously downloaded all the hourly solar wind data described in section 2 of the manuscript. We calculated the hourly average values for each solar phase of the data. It should be noted that there are dates for which the solar wind parameters are poorly recorded. These dates are not taken into account in our study. Only situations where all data are simultaneously available have been used in this work. The hourly and phase-averaged values of the magnetospheric convection electric field (MCEF) are calculated using the formula established by [17] (Equation (1) below) and validated by [18].

$$E_M = 0.13E_y + 0.09 \tag{1}$$

The magnetospheric convection electric field E_M represents the fraction of the E_y component of the frozen electric field in the solar wind transmitted to the inner magnetosphere. It is important to note that Equation (1) above is based on electron density measurements from the GEOS 1 and ISSEE 1 spacecraft, which allow the efficiency of this transmission to be studied on a case-by-case basis with an almost perfect correlation coefficient of 0.97.

3.4. Method for Determining the Energy Transmitted to the Magnetosphere

Magnetic reconnections followed by magnetospheric convection phenomena via solar winds enable energy transfer to the inner magnetosphere. This flow of energy transmitted to the inner magnetosphere results mainly from the magnetic interaction between the solar wind and the Earth's magnetosphere. One of the main problems in magnetospheric physics is understanding the transfer of energy from the solar wind to the magnetosphere. Several authors, such as [19]-[21], have proposed the magnetosphere solar wind dynamo as the probable mechanism for energy exchange between the solar wind and the magnetosphere. Several functions have been established to evaluate this energy.

Subsequently, in order to estimate the power transmitted to the inner magnetosphere during reconnection between interplanetary magnetic field (IMF) lines and geomagnetic lines, several coupling functions were formulated, such as those by [22]-[24]. It is important to note that the function established by [22], was improved by Akasofu three years later, in 1981, through more extensive studies. However, it is also important to note that most of these coupling functions have shortcomings related to the fact that they overestimate or underestimate the amounts of energy transmitted to the magnetosphere. Notwithstanding the shortcomings of the various coupling functions, it is now well known that the function that best approximates the energy flux transmitted to the inner magnetosphere under the impact of solar winds is that of [15] [25] [26], whose mathematical formulation is given by Equation (2) below.

$$E_{in} = 3.78\times10^{7} n^{0.24} v^{1.47} B_T^{0.86} \left[\sin^{2.70}\left(\frac{\theta}{2}\right) + 0.25 \right] \quad (2)$$

In this equation, E_{int} is expressed in W and evaluates the maximum energy transmitted per unit of time to the inner magnetosphere by solar winds, particularly the fast ones that are the subject of our investigation. The interplanetary parameters n, v, θ and B_T used in Equation (2) represent, respectively, the electron density in the solar wind (in cm^{-3}), the solar wind velocity in km/s, the clock angle of the IMF in the plane perpendicular to the Sun-Earth line in degrees, and the amplitude of the transverse magnetic field in nT.

Please note that:

$$B_T = \sqrt{B_x^2 + B_y^2} \quad (3)$$

and

$$\theta = \tan^{-1}\left(\frac{B_y}{B_z}\right) \quad (4)$$

In this research work, the function (Equation (2)) will be used to quantify the maximum energy penetrating the inner Earth magnetosphere.

4. Results and Discussion

4.1. Cross-Variability of MCEF and IMF-Bz Regardless of Solar Phases

The diurnal variations of the Bz component of the interplanetary magnetic field (IMF-Bz) and the magnetospheric convective electric field (MCEF), regardless of solar phases, are shown in Figure 2. This figure shows that when the MCEF tends to increase, the CMI-Bz decreases and vice versa: the two parameters evolve in opposite phases. It is important to note that the correlation coefficient between these two parameters is almost perfect: −0.98. A detailed analysis of the diurnal

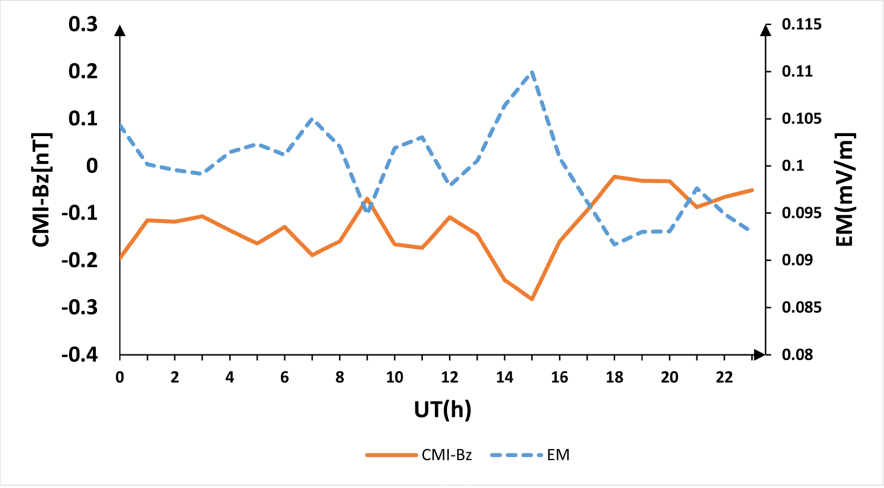

Figure 2. Daily variation of the MCEF (dotted curve) and IMF-Bz (solid curve) during solar cycle 24.

variability of the MCEF shows that it exhibits six trends regardless of the solar phase, including three increasing phases observed between 0300 UT - 0700 UT; 0900 UT - 1500 UT; 1800 UT - 2400 UT and three decreasing phases observed during the following time slots: 0000 UT - 0300 UT; 0700 UT - 0900 UT; 1500 UT - 1800 UT. The observed downward trends indicate a weakening of convection. This weakening could be explained by the maintenance of the Bz component of the CMI from south to north. According to [27] when the CMI is directed northwards, the interplanetary magnetic field lines and the geomagnetic field lines are parallel and any reconnection at the front of the magnetosphere is impossible. The energy accumulated inside the magnetosphere dissipates [28]. This dissipation of energy and matter leads to a decrease in the magnetospheric convection electric field. It is important to note that this interpretation corroborates those of [29] and [30], who found that magnetospheric convection weakens when the IMF shifts from south to north.

The three increasing phases observed indicate an increase in the magnetospheric convection electric field. These phases result from the IMF switching from a south-north direction to a north-south direction. According to [28] such a change in the direction of the IMF-Bz accentuates magnetospheric convection. Furthermore, periods of increase in the average hourly MCEF intensities could therefore be attributed to a reconnection between the antiparallel magnetic field lines of the south-oriented IMF-Bz and those of the Earth's magnetic field. Indeed, [31] noted that a north-south orientation of the IMF promotes magnetic reconnection, leading to an intensification of the magnetospheric convection electric field. It is important to note that the first two growing phases from 0300 UT to 0700 UT and from 0900 UT -1500 UT can be attributed respectively to reconnections at the nose of the magnetosphere and its lobes, and the increasing phase observed between 1800 UT and 2100 UT can be attributed to the consequences of night-time reconnection [32]. It is important to note that night-time reconnection is consistent with Dungey's reconnection theory (1961), according to which magnetic field lines open on the day side and close on the night side at the second neutral point. This process causes energy to accumulate in the tail of the magnetosphere, which causes the trapped particles to move towards the Earth, thus explaining the increase in magnetospheric convection observed in the night sector and, consequently, the increase in average MCEF intensities.

In order to refine our analyses of the influence of frozen IMF-Bz in fast solar winds on MCEF variability during solar cycle 24, we establish cross-correlations between these two parameters. **Table 2** presents these correlations as well as the slopes of IMF-Bz and MCEF. The last column of the table presents the ratio $\left|\frac{\Delta B_z}{\Delta E_M}\right|$. Nous remarquons que ce rapport quel que soit la plage d'heure concernée est supérieur à 1. This result shows that at all times, magnetic effects are very predominant in energy transfer phenomena between the magnetosphere and fast

solar winds compared to electrical effects. The highest values of the ratio $\left|\frac{\Delta B_z}{\Delta E_M}\right|$ are observed between 0000 UT and 0300 UT and between 1800 UT and 2400 UT, suggesting a greater contribution from magnetic effects in the morning and at night. It is important to note that these significant contributions are observed in the mornings and at night, which are times when daytime reconnections (reconnection at the nose of the magnetosphere) and night-time reconnections occur, resulting in a massive influx of mass, momentum and energy into the magnetosphere [33] [34]. This finding on the significant contribution of magnetic effects indirectly aligns with the findings of [27], for whom the transfer of solar wind energy to the Earth's magnetosphere is closely linked to the Bz component of the interplanetary magnetic field (IMF) and, thanks to a large-scale reconnection process on the day side, a fraction of the available solar wind energy is able to penetrate our magnetosphere. Finally, it is important to note that our results are also partly consistent with those of [35], who found that an increase in the amplitude of the Bz component of the IMF, as well as in the speed and density of the solar wind, are factors responsible for strong disturbances in geomagnetic activity; geomagnetic activities that have a strong impact on MCEF variability [36].

Table 2. Correlations between the various parameters of fast solar winds.

Universal time [hours]	Slope of [mV/m.s]	Slope of IMF [nT/s]	Correlation E_M and $IMF\text{-}B_z$	$\left\|\frac{\Delta B_z}{\Delta E_M}\right\|$
00:00-03:00	-1.60×10^{-3}	2.65×10^{-2}	−0.99	16.56
03:00-07:00	1.10×10^{-3}	-1.57×10^{-2}	−0.97	14.27
07:00-09:00	5.10×10^{-3}	6×10^{-2}	−0.99	11.76
09:00-15:00	1.9×10^{-3}	-2.72×10^{-2}	−0.99	14.31
15:00-18:00	−9.1	8.44×10^{-2}	−0.99	14.06
18:00-24:00	5×10^{-4}	-8.5×10^{-3}	−0.94	17

4.2. Cross-Variability of MCEF and IMF-Bz According to Different Solar Phases

The diurnal variations of the interplanetary magnetic field component Bz (IMF-Bz) and the magnetospheric convection electric field (MCEF) as a function of the different solar phases are shown in **Figure 3**. Panels (a), (b), (c) and (d) illustrate the variabilities of the MCEF and IMF-Bz respectively at the minimum phase, during the ascending phase, at the maximum phase and during the descending phase.

Analysis of these panels also shows that the E_M and Bz fields of solar origin evolve in opposition phase with very good correlations (r) for each phase of solar cycle 24: −0.97 for the solar minimum and maximum phases, −0.99 for the ascending phase, and −0.98 for the descending phase. These very good correlations

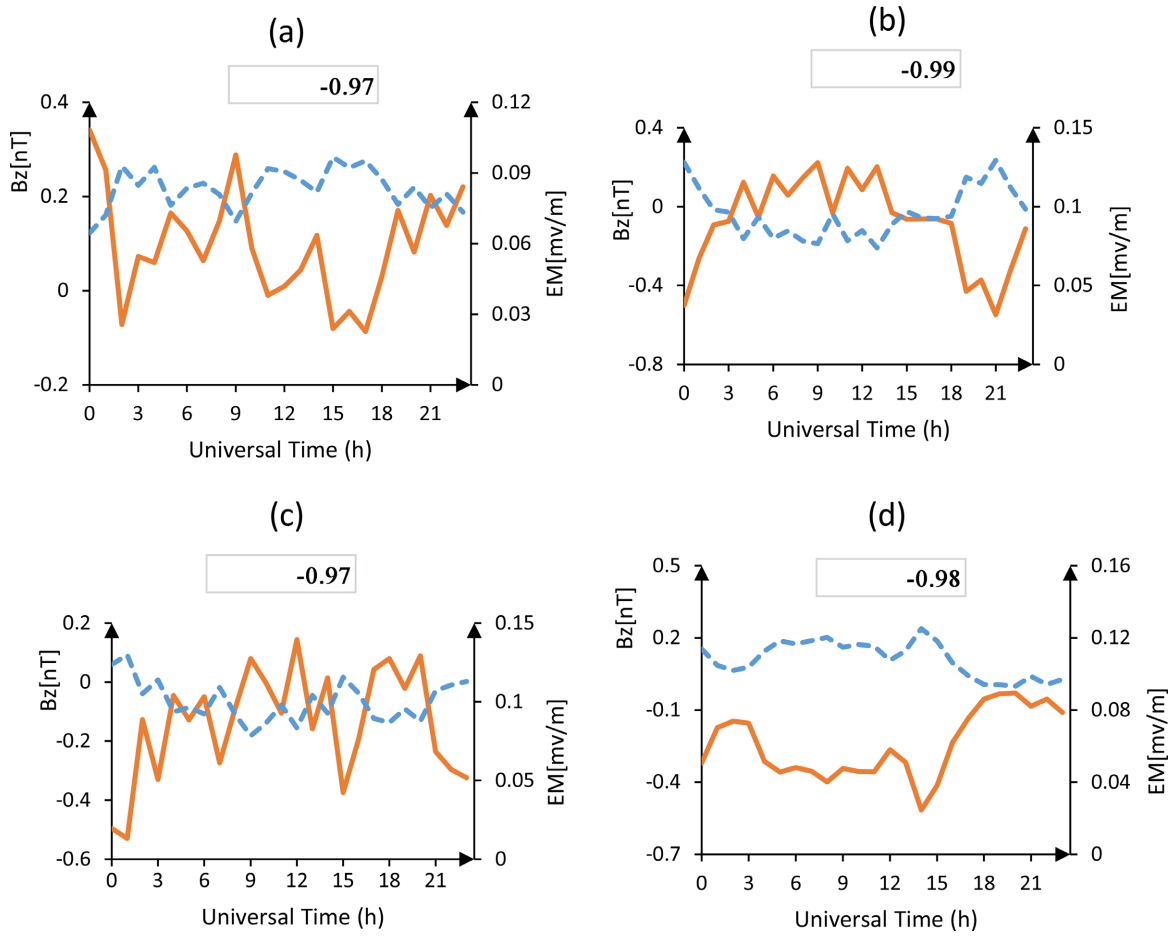

Figure 3. Variability of MCEF (dotted line) and IMF-Bz (solid line) as a function of the phases of solar cycle 24.

between the two fields show: (a) that the intensity of the MCEF is intrinsically linked to the IMF-Bz parameter of the solar wind, (b) the crucial importance of the Bz component of the IMF in the injection of charged particles from fast solar winds into the magnetosphere, (c) that the effectiveness of the interaction between fast solar winds and the Earth's magnetosphere is intrinsically linked to solar wind parameters.

Pearson coefficients, which are negative values tending towards −1: (a) reflect the protective nature of the magnetosphere against charged particles contained in the solar wind and (b) show that the MCEF and IMF-Bz under the action of geomagnetic storms evolve in opposite phase on a longer scale (solar cycle scale) than our scale (phase of a solar cycle) and are well correlated during solar cycle 24. These different results are in line with the results of previous work such as that of [37]-[39], for whom one of the key factors in fast solar winds from coronal holes or those accompanying ICME emissions, responsible for the development of the main phase of geomagnetic storms, would be the Bz component of the IMF (IMF-Bz). It is also important to note that the importance of the Bz component of the IMF in the injection of charged particles into the magnetosphere has also been supported in previous work such as that of [15] [40] [41].

4.3. Energy Dynamics of the Magnetosphere under the Influence of High-Speed Solar Wind

Table 3 shows the average values of the power transmitted to the inner magnetosphere and some parameters of fast solar winds during solar cycle 24. The six (06) time ranges adopted are derived from the IMF-Bz and MCEF variability curves shown in Figure 4.

Analysis of the last column of the table shows that for the phase minimum, energy transfer is greater between 0000 UT and 0300 UT, 0700 UT and 0900 UT, and 1500 UT and 1800 UT compared to the remaining time ranges. The maximum value of the power received (30 GW) is obtained between 0700 UT and 0900 UT and the lowest (2 GW) Pendant la phase ascendante la valeur maximale de la puissance est atteinte entre 0300 TU et 0700 TU (le matin) alors que la valeur minimale de la puissance transmise à la magnétosphère interne est observée dans l'intervalle de temps 1800 UT-2400UT. Aussi les valeurs de la puissance reçue sont plus importantes dans la matinée (0000 TU à 0900 TU) que dans la soirée et la nuit; mieux la puissance moyenne transmise à la magnétosphère interne croît de 0000 UT à 0900 UT et décroit continuellement jusqu'à 2400 UT.

During the maximum phase, the values of the received power are higher between 0000 UT and 1800 UT and become low at night (1800 UT to 2400 UT). Strong power transfers are observed between 0900 UT and 1500 UT and are of the order of 241 GW. The high power values observed in the morning and evening during this phase of maximum solar activity illustrate a more efficient transfer of energy in the morning and evening.

The energy values for the different time slots obtained during the descending phase are the most remarkable during solar cycle 24, the period under investigation. These values, except between 0000 UT and 0700 UT, are very high compared to those of the other three phases. Energy transfer during this declining phase of sunspot activity is less significant in the morning (0000 UT to 0700 UT) and becomes more crucial in part of the evening (1500 UT to 1800 UT) and during the night (1800 UT to 2400 UT). It should be noted that maximum power is obtained at night (18:00 UT and 24:00 UT) and is of the order of (1586 GW). Also during this phase of solar decline, high powers transmitted to the magnetosphere are observed in the morning between 07:00 UT and 09:00 UT.

It should be noted that during the ascending phase, the energy transmitted per unit of time to the inner magnetosphere is higher between 0000 UT and 1500 UT, a long period during which the IMF-Bz maintains a northward orientation, which is not favourable for magnetic reconnections that inject particles into the inner magnetosphere, than during the time period 1500 UT - 2400 UT, when the IMF-Bz is southward. Thus, in the time interval 1500 UT - 2400 UT, although the IMF-Bz is southward, an orientation favourable to magnetic reconnection, the power transmitted to the inner magnetosphere is relatively weaker compared to the northward orientation of the IMF-Bz during the same phase. A comparative analysis of the power transmitted to the inner magnetosphere during the rapid solar

wind-magnetosphere interaction during the maximum phase and the ascending phase reveals that at the maximum phase, although the IMF-Bz maintains a southward orientation at all times during said phase, the energy transmitted per unit time to the internal magnetosphere is lower than that transmitted to the internal magnetosphere during the ascending phase during the time intervals for which the IMF-Bz maintains a northward orientation. At first glance, these results suggest that during the active phase of solar cycle 24, energy transfers are more efficient when the IMF is oriented northward than southward. It is important to note that such energy transfers are generally the result of reconnections at the lobes of the magnetosphere, which occur between the initially north-oriented IMF lines and the Earth's magnetic field lines. However, it is also important to note that these large amounts of energy transmitted to the inner magnetosphere for these north-oriented IMF could come not only from magnetic reconnections, which are more efficient in terms of energy transmitted to the inner magnetosphere when the IMF is south-oriented [30] [33] [42], but also: (a) significant contributions of energy entering the magnetosphere through the polar cones, (b) abnormal diffusion of solar plasma energy towards the magnetopause, (c) a particularly high reconnection rate at the flanks of the magnetosphere during this phase, due to strong magnetic turbulence caused by the increase in the number of sunspots, which are regions where strong magnetic fields prevail. Analysis of **Table 3** also shows that for the same south orientation of the IMF-Bz component, magnetic reconnections are more efficient and lead to a massive influx of charged particles, mass and momentum during the descending phase than during the maximum phase. Similarly, magnetic reconnections occurring at the lobes of the magnetosphere [32], when the Bz component of the IMF is initially oriented northwards, are more effective during the ascending phase than during the maximum phase. These results show that, although it is well known that the south orientation of IMF-Bz is a necessary condition for reconnection, this parameter is not the only one to be taken into account in seeking to clarify magnetospheric dynamics in general and in assessing the energy transmitted to the Earth's magnetosphere in particular.

Furthermore, the various results we have obtained show that the evolution of the energy received per unit of time by the magnetosphere under the impact of fast solar winds was very complex during solar cycle 24, depending on the phase of the solar cycle and the different time intervals. This is because it is difficult to determine from our results whether the magnetosphere as a whole receives more energy in the morning, evening or night during the phases of the solar cycle. Despite this rather random nature of the energy dynamics of the magnetosphere, we note that, depending on the time ranges identified, the magnetosphere gains more energy during the descending phase, especially after 0900 UT, than during the other three phases. The phase during which the magnetosphere receives the least energy is the minimum phase. For the maximum phase, the transfer is greater in the morning and evening than at night (1800 UT to 2400 UT).

Table 3. Average values of power transmitted to the magnetosphere and some parameters of fast solar winds during Solar Cycle 24.

Phases	Universal Time UT (hour)	IMF-B_z	n [cm^{-3}]	V [km/s]	B_T [nT]	θ [in °]	E_{in} [GW]
Minimum	00:00-03:00	Nord	3.64	555.18	0.13	39.44	29
	03:00-07:00	Nord	3.52	557.41	0.007	2.06	2
	07:00-09:00	Nord	3.32	560.18	0.14	38.40	30
	09:00-15:00	Nord	3.07	559.27	0.08	18.45	16
	15:00-18:00	Nord	2.77	559.08	0.09	62.37	28
	18:00-24:00	Nord	2.67	554.80	0.04	6.35	8
Ascending	00:00-03:00	Nord	2.91	555.04	2.81	81.98	733
	03:00-07:00	Nord	2.73	557.62	2.77	88.50	790
	07:00-09:00	Nord	2.66	555.29	2.76	84.63	735
	09:00-15:00	Nord	2.68	554.34	2.40	86.51	670
	15:00-18:00	Sud	2.69	549.72	2.35	87.28	658
	18:00-24:00	Sud	2.70	546.16	2.45	78.55	593
Maximum	00:00-03:00	Sud	3.77	536.45	0.96	62.04	215
	03:00-07:00	Sud	3.44	537.77	0.81	74.94	224
	07:00-09:00	Sud	3.24	537.58	0.76	80.93	229
	09:00-15:00	Sud	3.09	535.01	0.77	84.61	241
	15:00-18:00	Sud	2.88	529.17	0.84	80.58	236
	18:00-24:00	Sud	2.80	525.22	0.52	81.71	156
Descending	00:00-03:00	Sud	4.62	550.05	1.6	71.51	423
	03:00-07:00	Sud	4.43	551.58	2.9	61.24	596
	07:00-09:00	Sud	4.22	552.60	9.8	54.32	1513
	09:00-15:00	Sud	3.88	551.80	6.5	54.44	1042
	15:00-18:00	Sud	3.75	549.20	7.1	70.55	1423
	18:00-24:00	Sud	3.73	545.65	6.2	84.19	1549

Figure 4 below shows the histogram of the average daily values of energy transmitted per unit of time to the inner magnetosphere by fast solar winds during the different phases of solar cycle 24. Analysis of this figure shows that the power transmitted to the inner magnetosphere is minimal at the minimum phase and maximal during the descending phase of the solar cycle. It is important to note that the average daily value of the power transmitted to the inner magnetosphere is higher during the ascending phase than that obtained during the phase maximum: the magnetosphere receives more energy during the ascending phase than

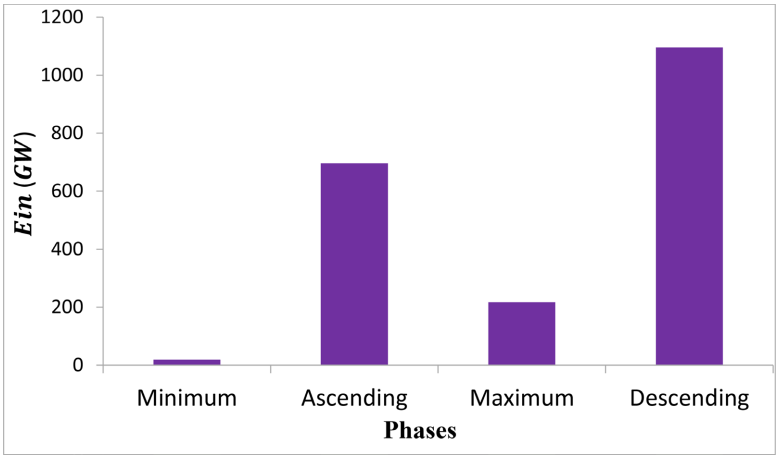

Figure 4. Average power transmitted to the magnetosphere as a function of the phases of solar cycle 24.

during the phase maximum. This result indirectly aligns with that of [43] for whom the transfer of energy between the Earth's magnetosphere and solar winds is more efficient during the phase maximum than during the minimum. The high speeds observed at the end of the solar cycle, characteristic of fast solar wind currents originating from coronal holes and triggering intense geomagnetic activity [44] [45] would partly explain the particularly high values of power transmitted to the Earth's magnetosphere during the decay phase of sunspot activity. On the other hand, the high-speed, high-density plasma flows from coronal holes, which are predominant at the end of the solar cycle [46]-[48], coupled with recurrent reconnections, which are major drivers of storms, could explain the high values of power transmitted during the downturn phase.

Strong magnetic turbulence at the solar wind/magnetosphere interface could be: (a) responsible for transfers to the inner magnetosphere through the magnetopause, either by triggering magnetic reconnection [49] sources of strong energy injection into the inner magnetosphere, or (b) factors facilitating "abnormal" diffusion of solar wind plasma particles into the magnetosphere [50]. The effects of these more pronounced disturbances during phases of growth and decline in sunspot activity could be a plausible hypothesis to explain the high powers transmitted to the inner magnetosphere during the ascending and descending phases of solar cycle 24.

Finally, we note that the energy input during the descending phase (1096 GW) is twice that during the ascending phase (695 GW). This significant difference in the injection of energy into the inner magnetosphere shows that the power transmitted to the inner magnetosphere is not symmetrical with respect to sunspot activity. It is also important to note that, regardless of the solar phase, the average power transmitted to the inner magnetosphere during solar cycle 24 is around 507 GW.

5. Conclusions

In this article, we use a statistical approach to investigate the cross-variabilities of

the MCEF and IMF-Bz as a function of different solar phases and regardless of the phase during solar cycle 24. In this article, we also quantify, using the Ein parameter from Wang, 2014, the power transmitted to the inner magnetosphere during solar wind-magnetosphere interaction, taking into account sunspot activity and the orientation of the Bz component of the interplanetary magnetic field.

A study of the cross-variability of the magnetospheric convection electric field and the Bz component of the interplanetary electric field shows that the two fields evolve in opposition phase with very satisfactory correlations (r) for each phase of solar cycle 24: −0.97 for the solar minimum and maximum phases, −0.99 for the ascending phase, −0.98 for the descending phase, and for all types of phases. Furthermore, a detailed analysis of the diurnal variability of the MCEF and the value of the Bz component of the IMF during all types of phases shows that they exhibit six trends, including three rising phases observed between 0300 UT and 0700 UT; 0900 UT and 1500 UT; 1800 UT - 2400 UT and three decreasing phases observed during the following time slots: 0000 UT - 0300 UT; 0700 UT - 0900 UT and 1500 UT - 1800 UT. The study of the diurnal variability of the MCEF also shows that during rapid solar wind-magnetosphere interaction, there are two daytime reconnections occurring at 0300 UT and 0900 UT respectively at the nose and flanks of the magnetosphere, and one night-time reconnection occurring at 1800 UT.

Our investigations also show that at all times of the day, magnetic effects are very predominant in the phenomena of energy transfer between the magnetosphere and fast solar winds compared to electrical effects. The contributions of these magnetic effects are greater in the morning and at night.

The Eint parameter varies according to solar activity, but does not follow it: it is minimal at solar minimum and maximal during the descending phase. More precisely, the power transmitted to the inner magnetosphere is minimal at phase minimum (19 GW) and maximal during the descending phase (1096 GW). The power transmitted during the ascending phase (696 GW) is about three times that transmitted during the solar maximum (216 GW). Regardless of the solar phase, the power transmitted to the inner magnetosphere is about 506 GW.

During solar cycle 24, the Earth's magnetosphere was most disturbed during the descending phase between 1800 UT and 2400 UT, when it received the highest energy during this phase, while it was least disturbed during the solar cycle minimum between 0300 UT and 0700 UT, when the lowest energy transfer was recorded.

This study has shed light on the response of the electric field of magnetospheric convection when the magnetosphere is impacted by fast solar winds. This study also enabled us to quantify the energies transmitted per unit of time to the Earth's magnetosphere during its interaction with high-speed solar winds. Notwithstanding these results, we must acknowledge that one of the major weaknesses of this study is that it covers only a single solar cycle, cycle 24. We recognise that a study covering a longer period (1966 to 2018 - solar cycles 20-24) would lead to more credible results and therefore to results whose generalisation would be more

unanimously accepted. Better still, a comparative study of the energies transmitted to the inner magnetosphere during periods of calm and disturbed activity from 1966 (the year of the first measurements of solar wind data) to 2018 (the date marking the end of the last complete solar cycle), taking into account, among other things, the impact of the season, the solar phase, the dynamic pressure of high-speed solar wind on the magnetosphere, magnetic reconnections, and pre-existing conditions at the flank of the magnetosphere before the impact of HSSW, would provide a better understanding of the energy dynamics of the magnetosphere during geomagnetic disturbances.

Since the energy exchanged fundamentally determines how the solar wind drives magnetospheric activity, in our future research on the energy dynamics of the solar wind-magnetosphere system, we will seek to understand the conditions under which the highest power transfer rates occur.

Acknowledgements

The authors would like to thank the editor and reviewers for their kind comments, suggestions and constructive proposals, which have enabled us to improve the document. The authors would also like to extend special thanks to all the providers of data used in this work, namely OMNIweb at NASA's Goddard Space Flight Centre for solar wind data, and the Royal Observatory of Belgium for providing the number of sunspots.

Conflicts of Interest

The authors declare no conflicts of interest regarding the publication of this paper.

References

[1] Koskinen, H.E.J. and Kilpua, E.K.J. (2022) Particle Source and Loss Processes. In: *Physics of Earth's Radiation Belts*, Springer, Cham.

[2] Zhang, J., Dere, K.P., Howard, R.A. and Bothmer, V. (2003) Identification of Solar Sources of Major Geomagnetic Storms between 1996 and 2000. *The Astrophysical Journal*, **582**, 520-533. https://doi.org/10.1086/344611

[3] Bamba, Y., Inoue, S. and Imada, S. (2020) Intrusion of Magnetic Peninsula toward the Neighboring Opposite-Polarity Region That Triggers the Largest Solar Flare in Solar Cycle 24. *The Astrophysical Journal*, **894**, Article 29. https://doi.org/10.3847/1538-4357/ab85ca

[4] Kusano, K., Ishii, M., Berger, T., Miyoshi, Y., Yoden, S., Liu, H., *et al.* (2021) Special Issue "Solar–terrestrial Environment Prediction: Toward the Synergy of Science and Forecasting Operation of Space Weather and Space Climate". *Earth, Planets and Space*, **73**, Article No. 198. https://doi.org/10.1186/s40623-021-01530-0

[5] Sawadogo, S., Gnabahou, D.A., Pahima, T. and Ouattara, F. (2024) Solar Activity: Towards a Standard Classification of Solar Phases from Cycle 1 to Cycle 24. *Advances in Space Research*, **73**, 1041-1049. https://doi.org/10.1016/j.asr.2023.11.011

[6] Chafik, B., El Malki, M., Miskane, F. and Nebdi, H. (2024) Study of Geomagnetic Activity According to kp Index and Its Variability in Relation to Sunspots over the Last Five Solar Cycles. *International Journal on "Technical and Physical Problems of*

Engineering", **16**, 331-341.

[7] Ouédraogo, P., Guibula, K., Diabaté, A., Fleury, R. and Ouattara, F. (2024) Study of Regular Variations in Vertical Total Electron Content (VTEC) from 2013 to 2021 at Station BF01 in Ouagadougou. *Current Journal of Applied Science and Technology*, **43**, 103-117. https://doi.org/10.9734/cjast/2024/v43i74410

[8] Kaboré, S., Segda, A.K., Gyébré, A.M.F. and Ouattara, F. (2024) Statistical Study of the Occurrence of Coronal Mass Ejections (CMEs) from 1996 to 2018 (Solar Cycles 23-24). *Journal of Modern Physics*, **15**, 2238-2255. https://doi.org/10.4236/jmp.2024.1512091

[9] Lindblad, B.A. and Lundstedt, H. (1981) A Catalogue of High-Speed Plasma Steams in the Solar Wind. *Solar Physics*, **74**, 197-206. https://doi.org/10.1007/bf00151290

[10] Intriligator, D. (1973) High Speed Streams in the Solar Wind. Report UAG-27, World Data Center A for Solar-Terrestrial Physics, Boulder. https://repository.library.noaa.gov/view/noaa/10222/noaa_10222_DS1.pdf

[11] Intriligator, D. (1977) The Large-Scale and Long-Term Evolution of the Solar Wind Speed Distribution and High Speed Streams. In: Shea, M.A., Smart, D.F., Wu, S.T., Eds., *Study of Travelling Interplanetary Phenomena*/1977, D. Reidel Publishing, 195-225.

[12] Tsurutani, B.T., Gonzalez, W.D., Gonzalez, A.L.C., Guarnieri, F.L., Gopalswamy, N., Grande, M., *et al.* (2006) Corotating Solar Wind Streams and Recurrent Geomagnetic Activity: A Review. *Journal of Geophysical Research*: *Space Physics*, **111**, A07S01. https://doi.org/10.1029/2005ja011273

[13] Hajra, R., Tsurutani, B.T., Brum, C.G.M. and Echer, E. (2017) High-Speed Solar Wind Stream Effects on the Topside Ionosphere over Arecibo: A Case Study during Solar Minimum. *Geophysical Research Letters*, **44**, 7607-7617. https://doi.org/10.1002/2017gl073805

[14] Tsurutani, B.T., Hajra, R., Tanimori, T., Takada, A., Remya, B., Mannucci, A.J., *et al.* (2016) Heliospheric Plasma Sheet (HPS) Impingement onto the Magnetosphere as a Cause of Relativistic Electron Dropouts (REDs) via Coherent EMIC Wave Scattering with Possible Consequences for Climate Change Mechanisms. *Journal of Geophysical Research: Space Physics*, **121**, 10130-10156. https://doi.org/10.1002/2016ja022499

[15] Gnanou, I., Gyébré, A.M.F., Guibula, K., Zoundi, C. and Ouattara, F. (2022) Energetic Dynamics of the Inner Magnetosphere in Contact with Fast Solar Wind Currents: Case of the Period 1964-2009. *International Journal of Geosciences*, **13**, 329-348. https://doi.org/10.4236/ijg.2022.135018

[16] Obridko, V.N., Shibalova, A.S. and Sokoloff, D.D. (2024) Gnevyshev Gap in the Large-Scale Magnetic Field. *Solar Physics*, **299**, Article No. 60. https://doi.org/10.1007/s11207-024-02292-0

[17] Lei, W., Gendrin, R., Higel, B. and Berchem, J. (1981) Relationships between the Solar Wind Electric Field and the Magnetospheric Convection Electric Field. *Geophysical Research Letters*, **8**, 1099-1102. https://doi.org/10.1029/gl008i010p01099

[18] Revah, I. and Bauer, P. (1982) Activity Report of the Research Center in Physics of the Terrestrial and Planetary Environment. Technical Note CRPE/115, 38-40. https://hal-lara.archives-ouvertes.fr/hal-02192225

[19] Siscoe, G.L. (1966) A Unified Treatment of Magnetospheric Dynamics with Applications to Magnetic Storms. *Planetary and Space Science*, **14**, 947-967. https://doi.org/10.1016/0032-0633(66)90132-2

[20] Axford, W.I. (1969) Magnetospheric Convection. *Reviews of Geophysics*, **7**, 421-459.

https://doi.org/10.1029/rg007i001p00421

[21] Akasofu, S.I. (1977) Physics of Magnetospheric Substorms. *Royal Astronomical Society*, *Quarterly Journal*, **18**, 170-187. https://adsabs.harvard.edu/full/1977QJRAS..18..170A

[22] Perreault, P. and Akasofu, S.I. (1978) A Study of Geomagnetic Storms. *Geophysical Journal International*, **54**, 547-573. https://doi.org/10.1111/j.1365-246x.1978.tb05494.x

[23] Gonzalez, W.D., Gonzalez, A.L.C. and Tsurutani, B.T. (1990) On the Equivalence of the Solar Wind Coupling Parameter E and the Magnetospheric Energy Output Parameter UT during Intense Geomagnetic Storms. *Planetary and Space Science*, **38**, 341-342. https://doi.org/10.1016/0032-0633(90)90099-c

[24] Finch, I. and Lockwood, M. (2007) Solar Wind-Magnetosphere Coupling Functions on Timescales of 1 Day to 1 Year. *Annales Geophysicae*, **25**, 495-506. https://doi.org/10.5194/angeo-25-495-2007

[25] Wang, C., Han, J.P., Li, H., Peng, Z. and Richardson, J.D. (2014) Solar Wind-Magnetosphere Energy Coupling Function Fitting: Results from a Global MHD Simulation. *Journal of Geophysical Research: Space Physics*, **119**, 6199-6212. https://doi.org/10.1002/2014ja019834

[26] Lockwood, M. and McWilliams, K.A. (2021) On Optimum Solar Wind-Magnetosphere Coupling Functions for Transpolar Voltage and Planetary Geomagnetic Activity. *Journal of Geophysical Research*: *Space Physics*, **126**, e2021JA029946. https://doi.org/10.1029/2021ja029946

[27] Dungey, J.W. (1961) Interplanetary Magnetic Field and the Auroral Zones. *Physical Review Letters*, **6**, 47-48. https://doi.org/10.1103/physrevlett.6.47

[28] Kelley, M.C., Fejer, B.G. and Gonzales, C.A. (1979) An Explanation for Anomalous Equatorial Ionospheric Electric Fields Associated with a Northward Turning of the Interplanetary Magnetic Field. *Geophysical Research Letters*, **6**, 301-304. https://doi.org/10.1029/gl006i004p00301

[29] Partamies, N., Juusola, I., Tanskanen, E., Kauristie, K., Weygand, J.M. and Ogawa, Y. (2011) Substorms during Different Phases. *Annales Geophysicae*, **29**, 2031-2043. https://doi.org/10.5194/angeo-29-2031-2011

[30] Kaboré, S., Gnabahou, D.A., Ouattara, F. and Zougmoré, F. (2019) Solar Cycle Phase and Magnetospheric Convection Electric Filed (MCEF) Time Variation from 1964 to 2009 under Shock Activity. *Journal of Earth and Environment Sciences*, **7**, Article 171.

[31] Rita, P., Oliveira, T. and Farisa, A. (2019) The Impact of E-Service Quality and Customer Satisfaction on Customer Behavior in Online Shopping. *Heliyon*, **5**, e02690. https://doi.org/10.1016/j.heliyon.2019.e02690

[32] Salfo, K., Inza, G., Karim, G. and Frédéric, O. (2025) Magnetospheric Convective Electric Field (MCEF): Comparative Diurnal Statistical Variability of Different Types of Shock and Magnetic Cloud Activity Days. *International Journal of Geosciences*, **16**, 189-203. https://doi.org/10.4236/ijg.2025.164010

[33] Russell, C.T. (2007) The Coupling of the Solar Wind to the Earth's Magnetosphere. In: *Space Weather—Physics and Effects*, Springer.

[34] Tenfjord, P., Hesse, M. and Norgren, C. (2018) The Formation of an Oxygen Wave by Magnetic Reconnection. *Journal of Geophysical Research*: *Space Physics*, **123**, 9370-9380. https://doi.org/10.1029/2018ja026026

[35] Arowolo, O.A., Akala, A.O. and Oyeyemi, E.O. (2021) Interplanetary Origins of Some

Intense Geomagnetic Storms during Solar Cycle 24 and the Responses of African Equatorial/Low-Latitude Ionosphere to Them. *Journal of Geophysical Research*: *Space Physics*, **126**, e2020JA027929. https://doi.org/10.1029/2020ja027929

[36] Kabore, S. and Ouattara, F. (2018) Magnetosphere Convection Electric Field (MCEF) Time Variation from 1964 to 2009: Investigation on the Signatures of the Geoeffectiveness Coronal Mass Ejections. *International Journal of Physical Sciences*, **13**, 273-281. https://doi.org/10.5897/ijps2018.4759

[37] Arnoldy, R.L. (1971) Signature in the Interplanetary Medium for Substorms. *Journal of Geophysical Research*, **76**, 5189-5201. https://doi.org/10.1029/ja076i022p05189

[38] Akasofu, S.I. (1981) Energy Coupling between the Solar Wind and the Magnetosphere. *Space Science Reviews*, **28**, 121-190. https://doi.org/10.1007/bf00218810

[39] Akasofu, S.I. (2019) Space Physics in the Earliest Days, as I Experienced. *Perspectives of Earth and Space Scientists*, **1**, e2019CN000116. https://doi.org/10.1029/2019cn000116

[40] O'Brien, T.P. and McPherron, R.L (2000) An Empirical Phase Space Analysis of Ring Current Dynamics: Solar Wind Control of Injection and Decay. *Journal of Geophysical Research*, **105**, 7707-7719.

[41] Akasofu, S.I. (2021) A Morphological Study of Unipolar Magnetic Fields and the Relationship with Sunspots. *Journal of Atmospheric and Solar-Terrestrial Physics*, **218**, Article 105625. https://doi.org/10.1016/j.jastp.2021.105625

[42] de Siqueira, P.M., de Paula, E.R., Muella, M.T.A.H., Rezende, L.F.C., Abdu, M.A. and Gonzalez, W.D. (2011) Storm-Time Total Electron Content and Its Response to Penetration Electric Fields over South America. *Annales Geophysicae*, **29**, 1765-1778. https://doi.org/10.5194/angeo-29-1765-2011

[43] Ahluwalia, H.S. (2000) Ap Time Variations and Interplanetary Magnetic Field Intensity. *Journal of Geophysical Research*: *Space Physics*, **105**, 27481-27487. https://doi.org/10.1029/2000ja900124

[44] Zerbo, J.L., Amory-Mazaudier, C. and Ouattara, F. (2013) Geomagnetism during Solar Cycle 23: Characteristics. *Journal of Advanced Research*, **4**, 265-274. https://doi.org/10.1016/j.jare.2012.08.010

[45] Poletto, G. (2013) Sources of Solar Wind over the Solar Activity Cycle. *Journal of Advanced Research*, **4**, 215-220. https://doi.org/10.1016/j.jare.2012.08.007

[46] Tsurutani, B.T., Gonzalez, W.D., Gonzalez, A.L.C., Tang, F., Arballo, J.K. and Okada, M. (1995) Interplanetary Origin of Geomagnetic Activity in the Declining Phase of the Solar Cycle. *Journal of Geophysical Research*: *Space Physics*, **100**, 21717-21733. https://doi.org/10.1029/95ja01476

[47] Echer, E., Alves, M.V. and Gonzalez, W.D. (2005) A Statistical Study of Magnetic Cloud Parameters and Geoeffectiveness. *Journal of Atmospheric and Solar-Terrestrial Physics*, **67**, 839-852. https://doi.org/10.1016/j.jastp.2005.02.010

[48] Salfo, K., Karim, G., Frederic, G.A.M. and Frederic, O. (2024) Statistical Study of the Occurrence of Coronal Holes in the Solar Corona during Solar Cycle 24. *Applied Physics Research*, **16**, 87-98. https://doi.org/10.5539/apr.v16n2p87

[49] Tenfjord, P. and Østgaard, N. (2013) Energy Transfer and Flow in the Solar Wind-Magnetosphere-Ionosphere System: A New Coupling Function. *Journal of Geophysical Research*: *Space Physics*, **118**, 5659-5672. https://doi.org/10.1002/jgra.50545

[50] Rezeau, L. (1999) La turbulence magnétique á l'interface vent solaire/magnétosphére. *Comptes Rendus de l'Académie des Sciences—Series IIB—Mechanics-Physics-Astronomy*, **327**, 299-311. https://doi.org/10.1016/s1287-4620(99)80069-6